J Periodont Res 2006; 41; 426–446

JOURNAL OF PERIODONTAL RESEARCH
doi:10.1111/j.1600-0765.2006.00884.x

Analysis of interleukin-1β-modulated mRNA gene transcription in human gingival keratinocytes by epithelia-specific cDNA microarrays

T. Steinberg[1], B. Dannewitz[2], P. Tomakidi[1], J. D. Hoheisel[3], E. Müssig[1], A. Kohl[1], M. Nees[4]

[1]Department of Orthodontics and Dentofacial Orthopedics, Dental School, [2]Section of Periodontology, Department of Operative Dentistry and Periodontology, Dental School, University of Heidelberg, Im Neuenheimer Feld 400, 69129 Heidelberg, Germany, [3]Deutsches Krebsforschungszentrum, Division of Functional Genome Analysis, Im Neuenheimer Feld 506, 69120 Heidelberg, Germany and [4]VTT Biotechnology, Itäinen Pitkäkatu 4, PO Box 106, FIN-20521 Turku, Finland

The first two authors have contributed equally to the manuscript.

Steinberg T, Dannewitz B, Tomakidi P, Hoheisel JD, Müssig E, Kohl A, Nees M. Analysis of interleukin-1β-modulated mRNA gene transcription in human gingival keratinocytes by epithelia-specific cDNA microarrays. J Periodont Res 2006; 41: 426–446. © Blackwell Munksgaard 2006.

Background/objectives: Proinflammatory cytokines such as interleukin-1β are known to be synthesized in oral gingivitis and periodontitis and lead to the activation of the transcription factor nuclear factor-κB (NF-κB). Although numerous effects of interleukin-1β on mesenchymal cells are known, e.g. up-regulation of intercellular adhesion moelcule-1 in endothelial cells, little is known of the effects of interleukin-1β on oral keratinocytes. The purpose of the present study was to seek interleukin-1β-mediated alterations in mRNA gene transcription and a putative activation of NF-κB in oral gingival keratinocytes.

Methods: As an *in vitro* model for gingivitis and periodontitis, immortalized human gingival keratinocytes (IHGK) were stimulated with the proinflammatory cytokine interleukin-1β. An epithelia-specific cDNA microarray was used to analyze mRNA expression profiles from IHGK cells treated with 200 units interleukin-1β/ml for 3, 6, 9, 12, and 24 h. Indirect immunofluorescence was carried out to detect NF-κB in IHGK following interleukin-1β treatment.

Results: Detailed analysis revealed distinct patterns of time-dependent changes, including genes induced or repressed early (3–6 h) or late (12–24 h) after interleukin-1β treatment. Differentially expressed genes were involved in (*i*) cell stress, (*ii*) DNA repair, (*iii*) cell cycle and proliferation, (*iv*) anti-pathogen response, (*v*) extracellular matrix turnover, and (*vi*) angiogenesis. A large number of genes were responsive to NF-κB and induction was concomitant with nuclear translocation of the p65 RelA subunit of NF-κB. Interestingly, many of these genes contain multiple NF-κB binding sites in their promoters.

Conclusion: Analysis of altered gene expression allows identification of gene networks associated with inflammatory responses. In addition to a number of well-known genes involved in gingivitis and periodontitis, we identified novel candidates that might be associated with the onset and maintenance of an inflammatory disease.

Thorsten Steinberg, Department of Orthodontics and Dentofacial Orthopedics, Dental School, University of Heidelberg, Im Neuenheimer Feld 400, 69120 Heidelberg, Germany
Tel: +49 0 622156 6581/56 – 6580
Fax: +49 0 622156 5753
e-mail: thorsten_steinberg@med.uni-heidelberg.de

Key words: cDNA arrays; mRNA gene transcription; inflammation; nuclear factor kappa-B; interleukin-1

Accepted for publication January 9, 2006

Interleukin-1α and interleukin-1β are involved in the pathogenesis of inflammatory diseases such as rheumatoid arthritis (1), inflammatory bowel disease, atherosclerosis (2), and periodontitis (3,4). Along with tumor necrosis factor-α, interleukin-1 receptor antagonist and interleukin-18, interleukin-1α and interleukin-β are multifunctional 'primary' cytokines (5). These play a central role in the regulation of acute inflammation and link the innate and acquired immune systems (6). In human keratinocytes, induction of interleukin-1 takes place upon stimulation with bacterial lipopolysaccharide, phorbol esters (12-*O*-tetradecanoyl phorbol 13-acetate, phorbol 12-myristate 13-acetate), physical or thermal injury, ultraviolet irradiation, and a variety of cytokines, i.e granulocyte–macrophage colony-stimulating factor, tumor necrosis factor-α, interleukin-6, transforming growth factor-α, including interleukin-1α and interleukin-1β themselves (7–10). Interleukin-1 also triggers chemotaxis of neutrophil granulocytes as well as T- and B-cell activation, (8). Interleukin-1-mediated signaling involves (*i*) activation of the nuclear transcription factor NF-κB (11), (*ii*) stimulation of the c-Jun N-terminal kinase and the p42/p44 and p38 mitogen-activated protein kinases (12), and activation of the activator protein 1 (AP-1) transcription factors (13). The major pathway activated by interleukin-1 appears to be through NF-κB, which requires the involvement of a number of regulatory proteins (11). Phosphorylation and proteolytic degradation of the inhibitory κB kinase complex I-κB (14) by IκB kinases releases functional NF-κB dimers, such as p50, p52, and p65 RelA, that translocate to the nucleus and activate the transcription of target genes. NF-κB regulates the expression of over 150 known target genes, among which the majority encodes for proteins involved in the regulation of cellular stress, immune response (15,16), and antipathogen response. These proteins include cytokines and chemokines like interleukin-6 and -8, or intercellular adhesion molecule-1 involved in neutrophil adhesion (17) and extravasations from blood vessels (18). Other proteins, like major histocompatibility complex class I-related chain A gene (MICA), are involved in antigen presentation (19) and function beyond the immediate immune response, e.g. the acute phase proteins interferon-γ and interleukin-18, which are required for the function of T helper type 1 cells (20). Most NF-κB target genes augment the capacity of cells to cope with cellular stress and support cell survival. For instance, NF-κB has been shown to inhibit apoptosis in a number of different cell types. In addition, recent findings have shown that NF-κB is involved in cell cycle control by induction of growth arrest in epithelial cells via the cyclin-dependent kinase inhibitor p21 (21). In the present study, an epithelia-specific cDNA microarray was used to investigate interleukin-1β-mediated alterations in mRNA gene expression in a human papillomavirus type 16 (HPV-16) E6/E7-immortalized human gingival keratinocytes cell line (IHGK), referring to experiments, demonstrating that E6/E7 has no effect on the interleukin-1β response in immortalized human keratinocytes (22). We used this cell line as an *in vitro* model system for gingivitis and periodontitis. Clustering of gene expression data for five different time-points of interleukin-1β treatment (3, 6, 9, 12, and 24 h) showed complex kinetics of differential mRNA expression for a large number of cellular genes, including novel, previously unknown NF-κB/interleukin-1β modulated genes. Our functional genomic approach contributes to the elucidation of gene networks involved in the onset and maintenance of inflammatory diseases, in particular gingivitis and periodontitis.

Materials and methods

Cell culture and stimulation

Human gingival keratinocytes (IHGK), immortalized with the HPV-16 E6/E7 oncogenes (23), were propagated under standardized cell culture conditions as previously described (24). Mass cell cultures were established to allow the performance of stimulation experiments using identical cell populations. For stimulation, cells were treated with 200 units of human recombinant interleukin-1β (Promocell, Heidelberg, Germany) for time periods of 3, 6, 9, 12, and 24 h, respectively. Non-stimulated cultures were used as controls.

Indirect immunofluorescence

For indirect immunofluorescence, IHGK were seeded on glass slides with at a density of 1×10^4 cells and grown until 75% confluency was reached. Cultures were fixed in ice-cold methanol (80%; 2 min; −20°C) and in acetone (3 min; −20°C) and then incubated overnight at 4°C in a humid chamber with an antibody directed against the 65-kDa subunit of the transcription factor NF-κB (Santa Cruz Biotechnology, Santa Cruz, CA, USA). After washing three times with phosphate-buffered saline, the secondary fluorochrome-coupled antibody (Chemicon, Hofheim/Taunus, Germany) was incubated for 1 h at room temperature. For total nucleus staining, samples were incubated with propidium iodide (Sigma, Munich, Germany; 0.5 μg/ml, 30 min). Finally, cell-coated slides were embedded in mounting medium (Vectashield, Vector, Weinheim, Germany), and the distribution of NF-κB-specific fluorescence signals in conjunction with propidium iodide nucleus staining was documented using a Leica confocal laser scan microscope (TCS NT CLSM; Leica, Bensheim, Germany).

RNA isolation

Total RNA from non-stimulated and stimulated cell cultures was isolated according to the TRIzol® one-step protocol (Invitrogen GmbH, Karlsruhe, Germany) including RNA precipitation using isopropanol. After precipitation, RNA was centrifuged and pellets were washed with 70% of ethanol and re-suspended in nuclease-free water. For further purification, RNA was selectively precipitated in the presence of 5 M lithium chloride at −20°C overnight. Finally, washed and dried pellets were dissolved in 40–50 μl nuclease-free water, and stored at −80°C.

Design of cDNA microarray

The primary intention was to generate an epithelia-specific cDNA microarray that addresses functional aspects of various epithelial and gastrointestinal tissues. Among others, these functional classes include genes, involved in epithelial differentiation (1200 genes), DNA repair and synthesis (170 genes), cell cycle control and proliferation (400 genes), apoptosis and response to chemotherapeutic drugs (200 genes), housekeeping (500 genes), and inflammation (400 genes). Furthermore, a number of genes differentially expressed in human epithelial cancers and precancers as well as inflammatory lesions were selected from serial analysis of gene expression (SAGE) libraries (http://www.ncbi.nih.gov/SAGE). Heterologous DNA from bacteriophage λ, virus sequences (HPV-16 and -18), and empty spots were used as negative controls. A total of 5200 different human cDNA clones, genes that represent 3500 individual genes (including many expressed sequence tags and hypothetical proteins), were selected from the IMAGE consortium clone collection. Clones were obtained from the Resource Center & Primary Database (RZPD) in Berlin, Germany.

Production of cDNA microarrays was performed essentially as described previously (25,26). DNA fragments were printed in duplicate at a 210-μm center-to-center spacing, with an average spot diameter between 90 and 110 μm.

Analysis of promoter regions

MatInspector (Genomatix Software GmbH, Munich, Germany) was used to analyze DNA fragments between 600 and 1000 nucleotides upstream of the transcription start site including TATA boxes, which were used to indicate functional promoter regions. MatInspector is a software tool that utilizes a large library of matrix descriptions for transcription factor binding sites to locate matches in sequences of up to 30,000 base pairs (27). For simplification, only NF-κB and AP-1 binding sites were investigated. NF-κB binding sites comprise five related sequences that are recognized by the different NF-κB complexes, i.e. the p50, p52, and p65/c-Rel subunits. In comparison, random sequences of 1000 nucleotides were screened and yielded on average between 0.1 and 0.3 NF-κB binding sites. For the majority of genes in clusters 1–4, classic promoter regions could be identified. For 58 of these, at least one NF-κB binding site was found. The average number of NF-κB binding sites per promoter region was 2.15. Genes with two or more binding sites are listed in Table 1.

Indirect fluorescent labeling, array hybridization, and array data processing

Labeling of cDNA probes for microarray hybridization was carried out as described elsewhere (28). Between 20 and 30 μg total RNA was denatured for 5 min at 70°C in 23 μl water. After chilling on ice, 4 μg Oligo-dT 20-mer primer (2 μg/μl), 8 μl of 5× first-strand reverse transcriptase (RT) buffer, 2 μl of a 20× nucleotide mix, 4 μl of 0.1 M dithiothreitol, 2 μl Superscript II reverse transcriptase (200 units/μl, Invitrogen, GmbH), and 1 μl Rnasin (20 units/μl, Promega Corporation, Madison, WI, USA) were added to a final volume of 40 μl. The 20× nucleotide labeling mix contained 80 mM aminoallyl-dUTP (Sigma, Munich, Germany), 120 mM dTTP, and 200 mM dGTP, dCTP, and dATP. RT buffer was incubated at 42°C for 120 min, and incubation was stopped by adding 5 μl of 500 mM EDTA. Remaining RNA was hydrolyzed by adding 10 μl of 1 M NaOH for 45–60 min at room temperature, followed

Table 1. Summary of functional gene promotors containing two to six nuclear factor-κB (NF-κB) binding sites

Abbreviation	Gene name	UniGene ID	NF-κB sites
ADPRT	ADP-ribosyltransferase	Hs.177766	2
CD163	CD163 antigen	Hs.74076	2
GATA1	GATA binding protein 1	Hs.765	2
GRO2	GRO2 oncogene	Hs.75765	2
HSPE1	heat-shock 10 kDa protein 1	Hs.1197	2
HXB	hexabrachion (tenascin C, cytotactin)	Hs.289114	2
IL10RB	interleukin-10 receptor, beta	Hs.173936	2
ITGAV	integrin, alpha V	Hs.295726	2
KIAA0100	KIAA0100 protein	Hs.151761	2
LGALS3	galectin 3	Hs.621	2
MMP2	matrix metalloproteinase 2	Hs.111301	2
MT1E	metallothionein 1E (functional)	Hs.74170	2
MYC	c-myc	Hs.79070	2
PISD	phosphatidylserine decarboxylase	Hs.8128	2
S100A9	calgranulin B	Hs.112405	2
SDCCAG43	serologically defined colon cancer antigen 43	Hs.132792	2
SON	SON DNA binding protein	Hs.92909	2
SPN	sialophorin (CD43)	Hs.80738	2
AIM2	absent in melanoma 2	Hs.105115	3
CHRNB4	cholinergic receptor, nicotinic, beta polypeptide 4	Hs.54397	3
EEF1G	eukaryotic translation elongation factor 1 gamma	Hs.2186	3
GJB2	connexin 26	Hs.323733	3
HSPA1A	heat-shock 70 kDa protein 1A	Hs.8997	3
HSPA1L	heat-shock 70 kDa protein 1-like	Hs.80288	3
HSPA2	heat-shock 70 kDa protein 2	Hs.75452	3
SCYB10	IP-10	Hs.2248	3
VEGF	vascular endothelial growth factor	Hs.73793	3
WDR1	WD repeat domain 1	Hs.85100	3
ZFP36	zinc finger protein 36, C3H type	Hs.343586	3
MPP2	membrane protein myristoylated 2	Hs.23205	4
SCYA20	small inducible cytokine subfamily A member 20	Hs.75498	4
CLDN5	claudin 5	Hs.110903	5
MAPK11	mitogen-activated protein kinase 11	Hs.57732	5
MYCN	N-myc	Hs.25960	5
SDC4	syndecan 4 (amphiglycan, ryudocan)	Hs.252189	6

by neutralization by adding 25 μl of 1 M sodium phosphate buffer (pH 7.5). The resulting cDNA was concentrated to a total volume of 9 μl (Microcon separators), and aminoallyl residues were chemically coupled to monofunctional Cy3- or Cy5-esters (Amersham BioSciences, Piscataway, NJ, USA). Then, 3 μM of lyophilized dyes were resuspended in 9 μl 0.1 M $NaHCO_3$ (pH 9), mixed with the cDNA, and incubated for 1 h at room temperature in the dark. The remaining dyes were quenched for 15 min using 9 μl of 4 M hydroxylamine. Labelled cDNA was purified using the QIAquick polymerase chain reaction (PCR) purification kit. For hybridization, cDNA was dissolved in 40 μl hybridization buffer containing 50% formamide, 3× saline sodium citrate (SSC), 1% sodium dodecyl sulfate, 5× Denhardt's reagent, and 5% dextran sulfate, 10 μg COT-1 DNA (Invitrogen GmbH), 8–10 μg polyA-DNA (Amersham Biosciences), and 4 μg yeast tRNA (Sigma) were added, denatured at 80°C for 10 min, and applied to the microarray. Hybridization was carried out for 16 h at 42°C in a humidified hybridization chamber. Slides were washed in 2× SSC, 0.1% sodium dodecyl sulfate for 2 min, followed by 1× SSC for 2 min, rinsed briefly in 0.2× SSC and dried by centrifugation at 500 r.p.m. for 5 min.

Array data processing

Detection of the fluorescent hybridization signals was performed using a ScanArray5000 laser scanner. Arrays were scanned at 5 μm resolution with variable photomultiplier tube voltage and laser intensity to obtain maximal signal intensities with < 1% saturated spots. Images for both the Cy3 and the Cy5 channels were merged and analyzed using the GENE PIX 4.0 software package. The intensity of array elements was measured as the mean of all pixels covered by an individual spot diameter. Local background was subtracted using the mean of the intensity of pixels directly surrounding each individual spot. Spots with low intensity (< 400 units), a spot size < 60 μm, or high background (ratio of signal to background < 2.5) were excluded from analysis unless the other channel was > 2000. A global normalization model was used to adjust intensities in the Cy3- and Cy5-fluorescence channels. Two or three identical array hybridizations were performed for each time-point, and data were combined (raw data). Cy3 and Cy5 dyes were swapped in duplicate experiments to exclude artifacts originating from the labeling process. Furthermore, two independent sets of experiments, starting with RNA from different cell cultures and individual RNA extractions, were used. For the second set of hybridizations (experiment 2), smaller arrays that contain only a subset of genes were used. Raw data were filtered for genes that were significantly changed above factor 1.0 within the 95% confidence interval ($P < 0.05$) for each experiment subset/time-point, and reproducibly changed by a ratio of at least two in any one given time-point of the interleukin-1β treatment. Data were logarithmically transformed (log base 2), and directly used for cluster analysis (29). Sorting of gene expression data was performed using the K-means algorithm, with seven preset clusters (Fig. 2A–D) and in tabular form with annotation software (EASE 2.0, National Institute of Health, USA) in Tables 2–8.

Reverse transcription polymerase chain reaction (RT-PCR)

Semiquantitative RT-PCR was essentially performed as previously described (30). For cDNA synthesis, 5–10 μg purified RNA were reverse transcribed for 1 h at 42°C in a total volume of 50 μl, containing 500 μM each of the four individual dNTPs; 10 mM dithiothreitol, 1.25 μM oligo-dT primer (T_{16-18}), 20–40 units RNasin (Promega), and 75 units Superscript Reverse Transcriptase II (Gibco) in 1× RT buffer. RT reactions were diluted 5–10-fold, and for each PCR 2 μl of diluted RT-mix were included. Amplifications were performed in a volume of 20 μl in 96-well plates using a Stratagene Robocycler, in the presence of 50–100 μM dNTPs, 0.5 μM of each oligonucleotide primer, 1.75 mM magnesium chloride, and 1 unit *Taq* DNA polymerase (Gibco). To exclude saturation or plateau effect of amplification and to optimize PCR conditions for each gene individually, PCR was repeated using a total number of 24, 27, 30, and 33 PCR cycles, respectively. Each reaction was performed at least twice using independent reverse transcription reactions to confirm reproducibility. Densitometric analysis of PCR experiments has been carried out with image analysis software IMAGEJ 2.0 and the mean pixel values are rectified above gel background and listed in Table 9.

Results

Interleukin-1β-mediated nuclear translocation of NF-κB

To demonstrate the activation of NF-κB in IHGK cultures upon stimulation with interleukin-1β, we analyzed time-dependent nuclear translocation of this transcription factor by using indirect immunofluorescence preceding treatment with 200 units interleukin-1β for 3, 6, 12, and 24 h, respectively. In accordance with a recently published study employing human foreskin keratinocytes immortalized with the HPV-16 E6 and E7 genes (31), in our untreated keratinocytes NF-κB was almost exclusively localized to the cytoplasm (Fig. 1A). In marked contrast, at 6 h, interleukin-1β treatment resulted in strong and clearly visible nuclear translocation of NF-κB. This is indicated in the overlay image by the yellow nuclear signal, which results from mixed red fluorescence in the nucleus (propidium iodide staining) and the green cortical fluorescence (NF-κB p65 subunit) inside the nucleus. Also notable is a strong localization of NF-κB at the nucleus–cytoplasm interface (Fig. 1B). NF-κB translocation to the nucleus in conjunction with the loss of green fluorescence in the cytoplasm typically indicates functional activation of the NF-κB transcription factor, which is retained in the cytoplasm as inactive complexes with I-κB proteins. NF-κB is actively transported into the nucleus upon rapid degradation of IκB protein. At 6 h of interleukin-1β treat-

Table 2. Genes listed to function from cluster analysis I (Fig. 2A)

Unigene ID	GO molecular function	Gene name	Official gene symbol
Hs.125244	ATP binding; DNA-dependent ATPase activity; damaged DNA binding	RAD51-like 3 (*S. cerevisiae*)	RAD51L3
Hs.20136	transcription factor activity	chromosome X open reading frame 6	CXorf6
Hs.35120	nucleotide binding, DNA binding, ATP binding, delta-DNA polymerase cofactor complex	replication factor C (activator 1) 4, 37 kDa	RCF4
Hs.74076	scavenger receptor activity, extracellular region integral to plasma membrane, antimicrobial humoral response (*sensu* Vertebrata)	CD163 antigen	CD163
Hs.79070	protein binding; transcription factor activity	v-myc myelocytomatosis viral oncogene homolog (avian)	MYC
Hs.20315	transferase activity	interferon-induced protein with tetratricopeptide repeats 1	IFIT1
Hs.252189	cytoskeletal protein binding	syndecan 4 (amphiglycan, ryudocan)	SDC4
Hs.2780	RNA polymerase II transcription factor activity; transcription factor activity	jun D proto-oncogene	JUND
Hs.105115	DNA binding	absent in melanoma 2	AIM2
Hs.2236	ATP binding; protein serine/threonine kinase activity; protein-tyrosine kinase activity	NIMA (never in mitosis gene a)-related kinase 3	NEK3
Hs.2248	cAMP-dependent protein kinase regulator activity; chemokine activity	chemokine (C-X-C motif) ligand 10, small inducible cytokine subfamily B	CXCL10
Hs.169274	transferase activity	interferon-induced protein with tetratricopeptide repeats 2 (FLJ31637)	IFIT2
Hs.77602	DNA binding; damaged DNA binding	damage-specific DNA binding protein 2, 48 kDa	DDB2
Hs.478553	ATP binding; ATP-dependent helicase activity; DNA binding; DNA helicase activity; RNA binding; mRNA binding; translation initiation factor activity	eukaryotic translation initiation factor 4A2	EIF4A2
Hs.77502	ATP binding; magnesium ion binding; methionine adenosyltransferase activity	methionine adenosyltransferase II, alpha	MAT2A
Hs.79339	IgE binding; sugar binding	lectin, galactoside-binding, soluble, 3 (galectin 3)	LGALS3
Hs.75498	chemokine activity; protein binding	chemokine (C-C motif) ligand 20, small inducible cytokine subfamily A member 20	**CCL20**
Hs.926	GTP binding; GTPase activity; antiviral response protein activity	myxovirus (influenza virus) resistance 2 (mouse)	MX2
Hs.111301	calcium ion binding; collagenase activity; gelatinase A activity; zinc ion binding	matrix metalloproteinase 2 (gelatinase A, 72 kDa gelatinase, 72 kDa type IV collagenase)	**MMP2**
Hs.73133	antioxidant activity; copper ion binding; electron transporter activity; zinc ion binding	metallothionein 3 (growth inhibitory factor (neurotrophic))	**MT3**
Hs.193716	carboxypeptidase A activity; complement component C3b receptor activity; copper\zinc superoxide dismutase activity; heavy metal binding	complement component (3b/4b) receptor 1, including Knops blood group system	**CR1**
Hs.154654	electron transporter activity; monooxygenase activity; oxygen binding; unspecific monooxygenase activity	cytochrome P450, subfamily 1B, polypeptide 1	**CYP1B1**
Hs.82085	plasminogen activator activity; protein binding; serine-type endopeptidase inhibitor activity	Plasminogen activator inhibitor type 1, serine (or cysteine) proteinase inhibitor, clade E, member 1	**SERPINE1**

Related genes in the results section have been grouped and highlighted with bold text.

ment, nuclear translocation of NF-κB reaches its maximum, and slowly re-distributes to the cytoplasm after this peak. This is concomitant with maximum activity of NF-κB-induced genes such as interleukin-8, as shown by the time–course experiments using cDNA microarray hybridizations. After 12 h of interleukin-1β treatment, partially cytoplasmic re-distribution of NF-κB is indicated by the abundance of green fluorescence within the cytoplasm (Fig. 1C), and after 24 h the re-distribution into the cytoplasm was almost complete (Fig. 1D), which is similar to

Table 3. Genes listed to function from cluster analysis II (Fig. 2A)

Unigene ID	GO molecular function	Gene name	Official gene symbol
Hs.102267	copper ion binding; protein-lysine 6-oxidase activity	lysyl oxidase	LOX
Hs.112405	calcium ion binding; signal transducer activity	S100 calcium binding protein A9 (calgranulin B)	S100A9
Hs.78996	DNA binding; DNA polymerase processivity factor activity; protein binding	proliferating cell nuclear antigen	PCNA
Hs.163724	degradation of G proteins via the proteosome	osteopetrosis associated transmembrane protein 1 (HSPC019 protein)	OSTMI
Hs.227789	ATP binding; MAP kinase kinase activity; protein serine/threonine kinase activity	mitogen-activated protein kinase-activated protein kinase 3	MAPKAPK3
Hs.25960	protein binding; transcription factor activity	v-myc myelocytomatosis viral related oncogene, neuroblastoma-derived (avian)	MYCN
Hs.74637	apoptosis inhibitor activity	testis enhanced gene transcript; testis enhanced gene transcript (BAX inhibitor 1)	TEGT
Hs.25960	protein binding; transcription coactivator activity	c-myc binding protein	MYCBP
Hs.8128	phosphatidylserine decarboxylase activity	phosphatidylserine decarboxylase	PISD
Hs.158303	ATP binding; DNA binding; tRNA ligase activity; transcription factor activity	PR domain containing 1, with ZNF domain	PRDM1
Hs.80738	binding; protein binding; transmembrane receptor activity	sialophorin (gpL115, leukosialin, CD43)	SPN
Hs.75981	cysteine-type endopeptidase activity; tRNA guanylyltransferase activity; ubiquitin thiolesterase activity; ubiquitin-specific protease activity	ubiquitin specific protease 14 (tRNA-guanine transglycosylase)	USP14
Hs.109646	NADH dehydrogenase (ubiquinone) activity; NADH dehydrogenase activity	NADH dehydrogenase (ubiquinone) 1 beta subcomplex, 6, 17 kDa	NDUFB6
Hs.110903	structural molecule activity	claudin 5 (transmembrane protein deleted in velocardiofacial syndrome)	CLDN5
Hs.79362	DNA binding; protein binding	retinoblastoma-like 2 (p130)	RBL2
Hs.23205	guanylate kinase activity; protein binding	membrane protein, palmitoylated 2 (MAGUK p55 subfamily member 2)	MPP2
Hs.25797	premRNA splicing factor activity	splicing factor 3b, subunit 4, 49 kDa	SF3B4
Hs.232116	ATP binding; protein serine/threonine kinase activity; protein-tyrosine kinase activity; tumor antigen	protein kinase, lysine deficient 2	PRKWNK2
Hs.16098	structural molecule activity	claudin 2	CLDN2
Hs.323733	connexon channel activity; protein binding	gap junction protein, beta 2, 26 kDa (connexin 26)	GJB2
Hs.74170	cadmium ion binding; copper ion binding; heavy metal ion transporter activity; helicase activity; zinc ion binding	metallothionein 1E (functional)	MT1E
Hs.57732	ATP binding; MAP kinase activity; MP kinase activity; protein-tyrosine kinase activity	mitogen-activated protein kinase 11	MAPK11
Hs.74034	structural molecule activity	caveolin 1, caveolae protein, 22 kDa	CAV1
Hs.765	ATP binding; protein binding; transcription factor activity	GATA binding protein 1 (globin transcription factor 1)	GATA1
Hs.808	RNA binding; nucleic acid binding	heterogeneous nuclear ribonucleoprotein F	HNRPF
Hs.27457	protein binding; nucleus; zinc ion binding; metal ion binding	BTB/POZ-zinc finger protein-like (ESTs)	APM1
Hs.177781	oxidoreductase activity	Carbonic reductase 4 (hypothetical protein MGC5618)	CBR4
Hs.351458	DNA binding; RNA binding; apoptosis regulator activity; structural molecule activity	THO complex 1 (p84)	THOC1
Hs.85100	actin binding	WD repeat domain 1	WDR1
Hs.325495	enzyme inhibitor activity; extracellular matrix (*sensu* Metazoa) metalloendopeptidase inhibitor activity	tissue inhibitor of metalloproteinase 2	TIMP2
Hs.288300	nucleic acid binding	zinc finger CCCH-type containing 12 A (FLJ23231)	ZC3H12 A
Hs.351990	chaperon activity	ESTs, Highly similar to CH60_HUMAN 60 kDa heat-shock protein, mitochondrial precursor (*H.sapiens*)	HSP60

Table 3. Continued

Unigene ID	GO molecular function	Gene name	Official gene symbol
Hs.352012	nucleotide binding, protein serine/threonine kinase activity, protein-tyrosine kinase activity, ATP binding, protein amino acid phosphorylation	WNK lysine deficient protein kinase 2 (serologically defined colon cancer antigen 43)	WNK2
Hs.334842	GTP binding; structural molecule activity	tubulin, alpha, ubiquitous	K-ALPHA-1
Hs.1197	ATP binding; cochaperonin activity; growth factor activity; heat-shock protein activity	heat-shock protein 1 (chaperonin 10)	**HSPE1**
Hs.80288	ATP binding; DNA binding; alternative-complement-pathway C3/C5 convertase activity; apoptosis inhibitor activity; heat-shock protein activity	heat-shock protein 1-like, 70 kDa	**HSPA1L**
Hs.1708	ATP binding; chaperone activity	chaperonin containing TCP1, subunit 3 (gamma); chaperonin	**CCT3**
Hs.54451	cell adhesion molecule activity; extracellular matrix structural constituent; heparin binding; protein binding; structural molecule activity	laminin, gamma 2	**LAMC2**

Related genes in the results section have been grouped and highlighted with bold text.

the non-stimulated situation (Fig. 1A). However, some small patches of positive NF-κB staining remain within the nuclei. This pattern coincides with gene expression data, indicating that activation of most directly NF-κB-regulated genes subsides after 12 h of interleukin-1β stimulation, although expression of some stress-related and interferon-induced genes continues. Our data indicate a stringent time-dependent control of NF-κB activation concomitant with the decrease of the cytokine-driven inflammatory response of the keratinocytes.

Microarray experiments

We used cDNA microarrays in two independent experiments to analyze gene expression altered by interleukin-1β treatment of IHGK cultures. As shown in Fig. 2(A,B), cluster analysis of gene expression data was performed separately for both experimental data sets (time points 3, 6, 9, and 12 h for experiment 1; 3, 6, and 24 h for experiment 2. A total of seven general classifications/clusters of differential mRNA gene expression were generated: four representing genes that are up-regulated in response to interleukin-1β (Fig. 2-A,B), and three clusters containing repressed genes (Fig. 2C,D). Different patterns of altered gene expression could be clearly identified, with kinetics that show peaks of up-regulation at 3 h (cluster I), 6 h (cluster II), and 12–24 h (cluster IV) after interleukin-1β application. Cluster III contains genes that are induced over a wide period of time (3–9 h).

Gene expression patterns

Of particular interest are genes induced early in response to interleukin-1β, which are represented by cluster I (Fig. 2A). Among these, a number of genes are causally related to mucosal inflammation, e.g. plasminogen activator inhibitor 1 (*SERPINE1*), matrix metalloproteinase 2 (*MMP2*), metallothionein 3 (*MT3*), complement component 3b/4b receptor (*CR1*), and dioxin-inducible cytochrome P450 (*CYP1B1*). Furthermore, genes indirectly associated with the inflammatory response, including extracellular matrix components, such as laminin α3 (*LAMA3*) and thrombospondin 1 (*THBS1*), are grouped in this cluster (Fig. 2A and Table 2; bold gene symbols). For instance, thrombospondin 1 promotes chemotaxis and haptotaxis of human peripheral blood monocytes (32). Similarly, some of the genes in cluster II are directly or indirectly associated with inflammation, including the extracellular matrix component laminin γ2 (*LAMC2*, kalinin or nicein), which has been described as a gene responsive to proinflammatory cytokines. However, most genes in cluster II belong to the large group of heat-shock proteins or chaperonins, for example heat-shock proteins *HSPE1*, *HSPA1L*, and chaperonin TCP1 subunit 3 (*CCT3*) (Fig. 2A and Table 3; bold gene symbols). Very similarly, clusters III and IV contain both inflammation-related genes as well as stress-induced proteins. In cluster III, the cytokines vascular endothelial growth factor-C and interleukin-8 are classic examples of a proinflammatory response (Fig. 2B and Table 4; bold gene symbols). The pivotal integrin αV (*ITGAV*), among other functions, mediates proinflammatory cytokine synthesis in human monocytes. Ornithine decarboxylase (*ODC1*) has been shown to be induced by bacterial lipopolysaccharide, a common inducer of inflammation (33). In cluster 4, inflammation-related genes include complement component 7 (*C7*), interleukin-10 receptor (*IL10RB*), and stromelysin 2 (*MMP10*) (Fig. 2C and Table 5; bold gene symbols).

Identification of NF-κB binding sites in promoter sequences of IL-1-induced genes

For all genes in clusters 1–4 (described above), upstream promoter regions were retrieved using the publicly available human genome databases (LocusLink at NCBI; http://www.ncbi.nlm.nih/LocusLink). Promoters lacking functional TATA and/or GC boxes were excluded. From a total of 58 functional gene promoters, 23 contained only one NF-κB-related

Table 4. Genes listed to function from cluster analysis III (Fig. 2B)

Unigene ID	GO molecular function	Gene name	Official gene symbol
Hs.289114	binding; cell adhesion receptor activity	tenascin C (hexabrachion)	TNC
Hs.256184	translation elongation factor activity	eukaryotic translation elongation factor 1 gamma	EEF1G
Hs.57301	ATP binding	mutL homolog 1, colon cancer, non-polyposis type 2 (*E. coli*)	MLH1
Hs.169531	ATP binding; ATP dependent RNA helicase activity; ATP dependent helicase activity; DNA helicase activity; RNA binding; RNA helicase activity	DEAD (Asp-Glu-Ala-Asp) box polypeptide 21	DDX21
Hs.40137	regulation of progression through cell cycle; ubiquitin cycle; mitosis cell division	anaphase promoting complex subunit 1	ANAPC1
Hs.117865	hydrogen\;sugar symporter-transporter activity	solute carrier family 17 (anion/sugar transporter), member 5	SLC17A5
Hs.92909	DNA binding; apoptosis inhibitor activity; double-stranded RNA binding; protein binding	SON DNA binding protein; Son cell proliferation protein	SON
Hs.183858	DNA binding; receptor binding; specific RNA polymerase II transcription factor activity; transcription coactivator activity; zinc ion binding	transcriptional intermediary factor 1	TIF1
Hs.2175	cell adhesion molecule activity; hematopoietin/interferon-class (D200-domain) cytokine receptor activity	colony stimulating factor 3 receptor (granulocyte)	CSF3R
Hs.54397	GABA-A receptor activity; acetylcholine receptor activity; extracellular ligand-gated ion channel activity; neurotransmitter receptor activity; nicotinic acetylcholine-activated cation-selective channel activity	cholinergic receptor, nicotinic, beta polypeptide 4	CHRNB4
Hs.624	chemokine activity; interleukin-8 receptor binding	interleukin 8	**IL8**
Hs.73793	DNA binding; growth factor activity; heparin binding; vascular endothelial growth factor receptor binding	vascular endothelial growth factor C	**VEGF**
Hs.295726	cell adhesion receptor activity	integrin, alpha V (vitronectin receptor, alpha polypeptide, antigen CD51)	**ITGAV**
Hs.75212	ornithine decarboxylase activity	ornithine decarboxylase 1	**ODC1**
Hs.2186	translation elongation factor activity protein biosynthesis	eukaryotic translation elongation factor 1 gamma	EEF1G
Hs.75765	chemokine activity	chemokine (C-X-C motif) ligand 2 (GRO2 oncogene)	CXCL2
Hs.77897	premRNA splicing factor activity	splicing factor 3a, subunit 3, 60 kDa	SF3A3
Hs.78919	amino acid transporter activity	Kell blood group precursor; Kell blood group precursor (McLeod phenotype)	XK
Hs.81361	DNA binding; DNA replication origin binding; RNA binding; mRNA binding	heterogeneous nuclear ribonucleoprotein A/B	HNRPAB
Hs.177766	DNA binding; NAD + ADP-ribosyltransferase activity; protein binding DNA repair	Poly (ADP-ribose) polymerase family, member 1 (ADP-ribosyltransferase)	PARP1
Hs.84883	extracellular region; lipid transport; lipid binding; lipoprotein metabolism	myosin phosphatase-Rho interacting protein (KIAA0864)	M-RIP
Hs.75452	ATP binding; heat shock protein activity; protein binding	heat-shock protein 2	**HSPA2**
Hs.36927	ATP binding; heat shock protein activity	heat-shock 105 kDa/110 kDa protein 1	**HSPH1**
Hs.8997	ATP binding; protein folding; response to unfolded protein	heat-shock 70 kDa protein 1 A	**HSPA1A**
Hs.80288	ATP binding; DNA binding; alternative-complement-pathway C3/C5 convertase activity; apoptosis inhibitor activity; heat shock protein activity	heat-shock 70 kDa protein 1-like	**HSPA1L**

Related genes in the results section have been grouped and highlighted with bold text.

binding site (data not shown). However, the majority, i.e. 35 promoters, contained between two and six binding sites. Table 1 summarizes the 35 promoters with a minimum of two binding sites for NF-κB-related transcription factors (c-Rel; RelB; p50 (NF-κB1); p52 (NF-κB2); and p65 (RelA).

Table 5. Genes listed to function from cluster analysis IV (Fig. 2B)

Unigene ID	GO molecular function	Gene name	Official gene symbol
Hs.133207	ATP binding; DNA binding; integrase activity; molecular_function unknown; protein binding; tRNA ligase activity	PTPRF interacting protein, binding protein 1 (liprin beta 1)	PPFIBP1
Hs.74578	nucleotide binding; DNA binding; double-stranded RNA binding; ATP-dependent DNA helicase activity;	DEAH (Asp-Glu-Ala-His) box polypeptide 9 ATP-dependent RNA helicase activity	DHX9
Hs.14732	electron transporter activity; malate dehydrogenase (decarboxylating) activity; malate dehydrogenase (oxaloacetate-decarboxylating) (NADP +) activity	malic enzyme 1, NADP(+)-dependent, cytosolic	ME1
Hs.9700	cyclin-dependent protein kinase regulator activity; kinase activity; protein binding	cyclin E1	CCNE1
Hs.24969	GABA-A receptor activity; extracellular ligand-gated ion channel activity	gamma-aminobutyric acid (GABA) A receptor, alpha 5;	GABRA5
Hs.3254	RNA binding; structural constituent of ribosome	mitochondrial ribosomal protein L23	MRPL23
Hs.77597	regulation of progression through cell cycle; nucleotide binding; protein serine/threonine kinase activity; protein-tyrosine kinase activity; protein binding	polo-like kinase	PLK1
Hs.349695	GTP binding; structural constituent of cytoskeleton	tubulin, alpha 2	TUBA2
Hs.75318	nucleotide binding; GTPase activity; structural molecule activity; GTP binding; microtubule	tubulin, alpha 1	TUBA1
Hs.159154	GTP binding; structural constituent of cytoskeleton	tubulin, beta, 4	TUBB4
Hs.152151	cell adhesion molecule activity; structural molecule activity	plakophilin 4	PKP4
Hs.82314	hypoxanthine phosphoribosyltransferase activity; magnesium ion binding	hypoxanthine phosphoribosyltransferase 1 (Lesch–Nyhan syndrome)	HPRT1
Hs.100000	calcium ion binding	S100 calcium binding protein A8 (calgranulin A)	S100A8
Hs.78802	ATP binding; cAMP-dependent protein kinase activity; glycogen synthase kinase 3 activity; protein binding; protein kinase CK2 activity; protein-tyrosine kinase activity	glycogen synthase kinase 3 beta	GSK3B
Hs.11482	DNA binding; premRNA splicing factor activity	splicing factor, arginine/serine-rich 11	SFRS11
Hs.300711	anticoagulant activity; calcium ion binding; calcium-dependent phospholipid binding; phospholipase inhibitor activity	annexin A5	ANXA5
Hs.343586	DNA binding; single-stranded RNA binding	zinc finger protein 36, C3H type, homolog (mouse)	ZFP36
Hs.78065	complement activity	complement component 7	**C7**
Hs.2258	collagenase activity; stromelysin 2 activity; zinc ion binding	matrix metalloproteinase 10 (stromelysin 2)	**MMP10**
Hs.173936	interleukin-10 receptor activity	interleukin 10 receptor, beta	**IL10RB**
Hs.151761	transporter activity	KIAA0100 gene product	KIAA0100
Hs.129548	DNA binding; RNA binding; heterogeneous nuclear ribonucleoprotein; protein binding	heterogeneous nuclear ribonucleoprotein K	HNRPK
Hs.180414	ATP binding; heat-shock protein activity; non-chaperonin molecular chaperone ATPase activity; protein binding	heat-shock 70 kDa protein 8	HSPA8
Hs.289088	ATP binding; heat-shock protein activity	heat-shock 90 kDa protein 1, alpha	HSPCA
Hs.1197	ATP binding; cochaperonin activity; growth factor activity; heat-shock protein activity	heat-shock 10 kDa protein 1 (chaperonin 10)	HSPE1
Hs.293678	Function unknown	mediator of RNA polymerase II transcription, subunit 25 homolog (yeast), hypothetical protein TCBAP0758	MED25

Related genes in the results section have been grouped and highlighted with bold text.

Table 6. Genes listed to function from cluster analysis V (Fig. 2D)

Unigene ID	GO molecular function	Gene name	Official gene symbol
Hs.141496	cell adhesion molecule activity; molecular_ function unknown	MAGE-like 2; melanoma antigen, family L, 2	MAGEL2
Hs.144700	ephrin receptor binding; transmembrane ephrin	ephrin B1	EFNB1
Hs.153704	ATP binding; protein serine/threonine kinase activity; protein-tyrosine kinase activity	NIMA (never in mitosis gene a)-related kinase 2	NEK2
Hs.156346	ATP binding; DNA binding; DNA topoisomerase (ATP-hydrolyzing) activity	topoisomerase (DNA) II alpha 170 kDa	TOP2A
Hs.171695	MAP kinase phosphatase activity; kinase activity; non-membrane spanning protein tyrosine phosphatase activity; receptor activity	dual specificity phosphatase 1	DUSP1
Hs.191356	DNA binding	general transcription factor IIH, polypeptide 2, 44 kDa	GTF2H2
Hs.298275	amino acid-polyamine transporter activity; transcription factor activity	solute carrier family 38, member 2, amino acid transporter 2	SLC38A2
Hs.226117	DNA binding	H1 histone family, member 0	H1F0
Hs.23960	cyclin-dependent protein kinase regulator activity; kinase activity; protein binding	cyclin B1	CCNB1
Hs.41587	3′-5′ exonuclease activity; ATP binding; ATP-binding cassette (ABC) transporter activity; single-stranded DNA specific endodeoxyribonuclease activity	RAD50 homolog (*S. cerevisiae*)	RAD50
Hs.25647	DNA binding; specific RNA polymerase II transcription factor activity; transcription factor activity	v-fos FBJ murine osteosarcoma viral oncogene homolog	FOS
Hs.334562	ATP binding; cyclin-dependent protein kinase activity; protein-tyrosine kinase activity	cell division cycle 2, G1 to S and G2 to M	CDC2
Hs.151734	protein transporter activity	nuclear transport factor 2	NUTF2
Hs.811	ubiquitin conjugating enzyme activity; ubiquitin-protein ligase activity	ubiquitin-conjugating enzyme E2B, RAD6 homology (*S. cerevisiae*)	UBE2B
Hs.143648	insulin receptor binding; receptor activity	insulin receptor substrate 2	IRS2
Hs.24641	binding; molecular_function unknown	cytoskeleton associated protein 2	CKAP2
Hs.663	ATP binding; ATP-binding and phosphorylation-dependent chloride channel activity; ATP-binding cassette (ABC) transporter activity; PDZ-domain binding; channel-conductance-controlling ATPase activity; chloride channel activity; cytoskeletal regulatory protein binding; ion channel activity	cystic fibrosis transmembrane conductance regulator, ATP-binding cassette (subfamily C, member 7)	CFTR
Hs.77204	ATP-binding cassette (ABC) transporter activity	centromere autoantigen F; 350/400 ka (mitosin)	CENPF
Hs.179526	enzyme inhibitor activity; protein binding; ribonuclease H activity	thioredoxin interacting protein	TXNIP
Hs.343586	DNA binding; single-stranded RNA binding	zinc finger protein 36, C3H type, homolog (mouse)	ZFP36
Hs.54943	protein translocase activity	fracture callus 1 homolog (rat)	FXC1
Hs.73090	transcription coactivator activity; transcription factor activity	nuclear factor of kappa light polypeptide gene enhancer in B-cells 2 (p49/p100)	NFKB2
Hs.74502	chymotrypsin activity; trypsin activity	chymotrypsinogen B1	CTRB1
Hs.90875	guanyl-nucleotide exchange factor activity; protein transporter activity; zinc ion binding	RAB interacting factor	RABIF
Hs.142827	function unknown	similar to Neuronal protein 3.1 (p311 protein) hypothetical protein LOC284361	LOC284361
Hs.620	actin binding; calcium ion binding; cell adhesion molecule activity; integrin binding; protein C-terminus binding; structural constituent of cytoskeleton	bullous pemphigoid antigen 1, 230/240 kDa	BPAG1
Hs.13999	transcription corepressor activity; transcription factor activity	SIN3 homolog B, transcriptional regulator (yeast), KIAA0700	SIN3B
Hs.111244	function unknown	Hypothetical protein LOC284361	LOC284361

Table 7. Genes listed to function from cluster analysis VI (Fig. 2C)

Unigene ID	GO molecular function	Gene name	Official gene symbol
Hs.153752	protein-tyrosine-phosphatase activity	cell division cycle 25 homolog B (*S. cerevisiae*)	CDC25B
Hs.174195	receptor signaling protein activity	interferon induced transmembrane protein 2(1–8D)	IFITM2
Hs.20315	transferase activity	interferon-induced protein with tetratricopeptide repeats 1	IFIT1
Hs.104222	GTP binding intracellular protein transport small GTPase mediated signal transduction	ADP-ribosylation factor-like 8B (hypothetical protein FLJ107222)	ARL10C
Hs.36	tumor necrosis factor receptor binding	lymphotoxin alpha (TNF superfamily, member 1)	LTA
Hs.8128	phosphatidylserine decarboxylase activity	phosphatidylserine decarboxylase	PISD
Hs.194562	DNA binding; protein binding	telomeric repeat binding factor (NIMA-interacting) 1	TERF1
Hs.2331	protein binding; transcription factor activity	E2F transcription factor 5, p130-binding	E2F5
Hs.146360	receptor signaling protein activity	interferon induced transmembrane protein 1 (9–27)	IFITM1
Hs.833	protein binding	interferon, alpha-inducible protein; (clone IFI-15K)	G1P2
Hs.89578	[RNA-polymerase]-subunit kinase activity; general RNA polymerase II transcription factor activity; transcription factor activity	general transcription factor IIH, polypeptide 1, 62 kDa	GTF2H1
Hs.265827	DNA binding	interferon, alpha-inducible protein (clone IFI-6–16)	G1P3
Hs.278613	DNA binding; molecular_function unknown	interferon, alpha-inducible protein 27	IFI27
Hs.8375	zinc ion binding	TNF receptor-associated factor 4	TRAF4
Hs.96	apoptosis regulator activity	phorbol-12-myristate-13-acetate-induced protein 1	PMAIP1

Confirmation of microarray expression data by semiquantitative RT-PCR

For selected genes, differential mRNA expression upon interleukin-1 stimulation was analyzed by semiquantitative RT-PCR, starting with RNA from the same samples that were also used for microarray analyses. Representative RT-PCR results are shown in Fig. 3(A). With few exceptions, modulation of mRNA expression could be demonstrated, showing variable kinetics of gene induction that ranged between early responses (3 h) and delayed genes (12–24 h). Furthermore, kinetics of induction closely corresponded to the original microarray expression data.

As shown in Fig. 3(B), mRNAs for the members of the matrix metalloproteinase gene family (MMPs) were induced by interleukin-1β with variable kinetics. For example, expression of MMP10 mRNA peaked at 9 h of treatment, which coincides with the microarray expression data, but MMP2 mRNA showed the highest transcription at 24 h after interleukin-1β treatment. However, semiquantitative RT-PCR clearly demonstrated interleukin-1β-dependent modulation of mRNA expression also for these genes. The results of these experiments have been corroborated by densitometric analysis (Table 9).

Discussion

Interleukin-1α and interleukin-β are among the most potent general mediators of immune reactions and inflammatory processes (34). The use of the cDNA microarray technology used in this study is an approach to elucidate a broad range of genes responsive to interleukin-1β in epithelial cells. The cDNA microarray used for this study has been specialized for the analysis of epithelial mRNA gene expression and contains a selection of 3500 human genes and expressed sequence tags. We were able to identify a large number of genes that are significantly up- or down-regulated in human gingival keratinocytes in response to the pro-inflammatory cytokine interleukin-1β. Interleukin-1β has been shown to be highly expressed in oral epithelia, including the human gingiva, in particular persisting oral inflammatory diseases such as gingivitis and periodontitis (35). Analysis of altered mRNA gene expression is pivotal to elucidating the role of genes that participate in the initiation and maintenance of inflammation and inflammatory diseases of epithelial tissues such as the oral mucosa, and contributes to identifying potential novel targets for therapeutic intervention. Our studies show a significant increase in mRNA gene expression of genes mainly associated with (*i*) cell stress (20 genes), (*ii*) DNA repair (15 genes), (*iii*) cell cycle and proliferation (18 genes), (*iv*) antipathogen response (37 genes), (*v*) extracellular matrix turnover (19 genes), and (*vi*) angiogenesis (six genes). Of the clones represented on the cDNA microarray, 259 responded to interleukin-1β, which corresponds to a total of 227 different human genes and 6.5% of the 3500 genes on the microarray showed an average differential expression in at least one time-point by a factor of more than twofold. Many of these

Table 8. Genes listed to function from cluster analysis VII (Fig. 2D)

Unigene ID	GO molecular function	Gene name	Official gene symbol
Hs.83126	DNA binding; general RNA polymerase II transcription factor activity; protein binding	TAF11 RNA polymerase II, TATA box binding protein (TBP)-associated factor, 28 kDa	TAF11
Hs.1376	11-beta-hydroxysteroid dehydrogenase activity; 2\,3-dihydro-2\,3-dihydroxybenzoate dehydrogenase activity	hydroxysteroid(11-beta) dehydrogenase 2	HSD11B2
Hs.169055	protein binding; Golgi stack	golgi autoantigen, golgin subfamily a, 2	GOLGA2
Hs.158287	cytoskeletal protein binding	syndecan 3 (N-syndecan)	SDC3
Hs.287820	cell adhesion molecule activity; collagen binding; extracellular matrix structural constituent; heparin binding; oxidoreductase activity	fibronectin 1	FN1
Hs.5338	carbonate dehydratase activity; zinc ion binding	carbonic anhydrase XII	CA12
Hs.23582	receptor activity	tumor-associated calcium signal transducer 2	TACSTD2
Hs.20295	ATP binding; protein serine/threonine kinase activity; protein-tyrosine kinase activity	CHK1 checkpoint homolog (S. pombe)	CHEK1
Hs.288936	structural constituent of ribosome	mitochondrial ribosomal protein L9	MRPL9
Hs.296323	ATP binding; cAMP-dependent protein kinase activity; protein kinase CK2 activity; protein serine/threonine kinase activity	serum/glucocorticoid regulated kinase	SGK
Hs.2979	defense response; digestion	trefoil factor 2 (spasmolytic protein 1)	TFF2
Hs.274382	nucleotide binding; double-stranded RNA binding; protein serine/threonine kinase activity; protein-tyrosine kinase activity	eukaryotic translation initiation factor 2-alpha kinase 2; interferon-induced, double-stranded RNA-activated protein kinase	EIF2AK2
Hs.82306	actin filament severing activity	destrin (actin depolymerizing factor)	DSTN
Hs.346868	G-protein coupled receptor activity\, unknown ligand; protein binding; rhodopsin-like receptor activity	EBNA1 binding protein 2	EBNA1BP2
Hs.23590	monocarboxylic acid transporter activity; symporter activity	solute carrier family 16 (monocarboxylic acid transporters), member 4	SLC16A4
Hs.112193	ATP binding; damaged DNA binding	mutS homolog 5 (*E. coli*)	MSH5
Hs.77910	hydroxymethylglutaryl-CoA synthase activity; lyase activity; transcription factor activity	3-hydroxy-3-methylglutaryl-Coenzyme A synthase 1	HMGCS1
Hs.333382	ubiquitin-protein ligase activity	WW domain containing E3 ubiquitin protein ligase 2, Nedd-4-like ubiquitin-protein ligase	WWP2
Hs.159263	adhesive extracellular matrix constituent; cell adhesion molecule activity; collagen; extracellular matrix structural constituent conferring tensile strength	collagen, type VI, alpha 2	COL6A2
Hs.198166	DNA binding; RNA polymerase II transcription factor activity; transcription coactivator activity; transcription factor activity	activating transcription factor 2	ATF2
Hs.79706	actin binding; structural constituent of cytoskeleton; structural constituent of muscle; structural molecule activity	plectin 1, intermediate filament binding protein 500 kDa	PLEC1
Hs.80684	transcription factor activity	high mobility group box 2	HMGB2
Hs.79141	growth factor activity	vascular endothelial growth factor C	VEGFC
Hs.180455	single-stranded DNA binding	RAD23 homolog A (*S. cerevisiae*)	RAD23A
Hs.44227	beta-glucuronidase activity; heparanase activity	heparanase	HPSE
Hs.101766	receptor activity	tansforming growth factor, beta receptor associated protein 1	TGFBRAP1
Hs.129872	MAP-kinase scaffold activity	sperm associated antigen 9	SPAG9
Hs.16131	cytokine activity; glucose-6-phosphate isomerase activity; growth factor activity	glucose phosphate isomerase	GPI
Hs.234279	microtubule binding; protein C-terminus binding	microtubule-associated protein, RP/EB family, member 1	MAPRE1
Hs.317	DNA binding; DNA topoisomerase type I activity	topoisomerase (DNA) I	TOP1
Hs.78865	DNA binding; general RNA polymerase II transcription factor activity; protein binding; transcription initiation factor activity	TAF6 RNA polymerase II, TATA box binding protein (TBP)-associated factor; TAF6 RNA polymerase II, TATA box binding protein (TBP)-associated factor, 80 kDa	TAF6
Hs.76932	ubiquitin conjugating enzyme activity; ubiquitin-protein ligase activity	cell division cycle 34	CDC34

Table 8. Continued

Unigene ID	GO molecular function	Gene name	Official gene symbol
Hs.1686	ATP binding; GTP binding; heterotrimeric G-protein GTPase activity; heterotrimeric G-protein GTPase\, alpha-subunit; signal transducer activity	guanine nucleotide binding protein (G protein), alpha 11 (Gq class)	GNA11
Hs.155421	beta-glucuronidase activity; carrier activity; nickel ion binding	alpha fetoprotein	AFP
Hs.82396	ATP binding; RNA binding; antiviral response protein activity; nucleotidyltransferase activity	2′,5′-oligoadenylate synthetase 1, 40/46 kDa	OAS1
Hs.345728	regulation of cell growth; protein kinase inhibitor activity; antiapoptosis; intracellular signaling cascade; JAK-STAT cascade	STAT induced STAT inhibitor 3; suppressor of cytokine signaling 3	SOCS3
Hs.80475	DNA binding; DNA-directed RNA polymerase II activity; DNA-directed RNA polymerase activity	polymerase (RNA) II (DNA directed) polypeptide J,13.3 kDa	POLR2J FGF7
Hs.54457	DNA binding; protein binding	CD81 antigen (target of antiproliferative antibody 1)	CD81
Hs.78060	calmodulin binding; phosphorylase kinase activity; phosphorylase kinase regulator activity	phosphorylase kinase beta	PHKB
Hs.95910	function unknown	G0/G1switch 2 putative lymphocyte G0/G1 switch gene	G0S2
Hs.284245	tRNA ligase activity	hypothetical protein IMPACT	IMPACT
Hs.170198	structural constituent of ribosome	likely ortholog of chicken chondrocyte protein with a poly proline region	
Hs.78050	cysteine protease inhibitor activity	small acidic protein	SMAP
Hs.211573	protein binding; structural molecule activity	heparan sulfate proteoglycan 2 (perlecan)	HSPG2
Hs.114316	alpha-*N*-acetylneuraminate alpha-2\,8-sialyltransferase activity	sialyltransferase 8 (alpha-2, 8-sialyltransferase) C	SIAT8C
Hs.279789	regulation of progression through cell cycle histone deacetylase complex; histone deacetylase activity	histone deacetylase 3	HDAC3
Hs.194685	DNA topoisomerase type I activity DNA topological change; DNA unwinding; DNA modification	topoisomerase (DNA) III beta	TOP3B
Hs.150477	3′-5′ exonuclease activity; ATP binding; ATP dependent helicase activity; DNA binding; DNA helicase activity; protein binding	Werner syndrome; Werner syndrome homolog (human)	WRN
Hs.156114	Immunoglobulin-like cell surface receptor for CD47, adhesion of cerebellar neurons	Protein tyrosine phosphatase, non-receptor type substrate 1	PTPNS1
Hs.240443	Function unknown	Homo sapiens cDNA: FLJ23538 fis	FLJ23538
Hs.340524	Function unknown	Transcribed locus, moderately similar to XP_511180.1 PREDICTED: similar to KIAA1049 protein [*Pan troglodytes*], ESTs	
Hs.205748	Function unknown	ESTs, Weakly similar to hypothetical protein FLJ20378 [*Homo sapiens*]	
Hs.100895	Function unknown	male sterility domain containing 1, hypothetical protein FLJ10462	MLSTD1
Hs.29052	Function unknown	fetal globin-inducing factor, hypothetical protein FLJ20189	FGIF
Hs.283742	Function unknown	Similar to chromosome 6 open reading frame 216 isoform 2; spinal muscular atrophy candidate gene 3-like, *H. sapiens* mRNA for retrotransposons	
Hs.146393	endoplasmic reticulum membrane; protein modification; response to unfolded protein; integral to membrane	homocysteine-inducible, endoplasmic reticulum stress-inducible, ubiquitin-like domain member 1	HERPUD1
Hs.333382	ubiquitin ligase complex, ubiquitin-protein ligase activity protein binding, ubiquitin cycle	WW domain containing E3 ubiquitin protein ligase 2, Nedd-4-like ubiquitin-protein ligase	WWP2
Hs.346868	ribosome biogenesis	EBNA1 binding protein 2	EBNA1BP2
Hs.234279	regulation of progression through cell cycle; microtubule; mitosis microtubule binding; protein C-terminus binding	Microtubule-associated protein, RP/EB family, member 1	MAPRE1

Table 9. Densitometric analysis of semiquantitative polymerase chain reaction experiments (Fig. 3A,B)

Interleukin-1β treatment	Gene Symbol	Mean pixel values	Mean pixel values	Gene symbol
Untreated	ME	12.120	26.879	FGF7
3 h		35.529	32.528	
6 h		38.300	33.126	
9 h		50.922	33.974	
12 h		60.978	48.518	
24 h		44.273	81.933	
Untreated	ZFP36	16.848	14.810	LOC5618
3 h		35.346	59.180	
6 h		49.344	33.780	
9 h		66.502	19.654	
12 h		56.915	17.331	
24 h		72.588	13.859	
Untreated	SRKP1	19.366	17.725	LAMA3
3 h		28.703	32.025	
6 h		44.634	35.593	
9 h		61.138	30.134	
12 h		57.722	28.907	
24 h		55.121	31.752	
Untreated	HSPA1A	149.022	10.534	IL-8
3 h		145.115	37.663	
6 h		138.026	41.514	
9 h		136.593	43.774	
12 h		138.508	31.690	
24 h		162.438	38.778	
Untreated	HSPA8	43.221	10.292	VEGF
3 h		62.292	23.678	
6 h		82.497	27.995	
9 h		83.062	19.866	
12 h		73.641	7.921	
24 h		46.621	7.162	
Untreated	SLC17A5	42.504	4	TNFAIP3
3 h		60.990	34.471	
6 h		80.133	46.988	
9 h		81.743	41.733	
12 h		71.432	27.902	
24 h		45.573	23.967	
Untreated	LTA	60.471	3.269	PAI1
3 h		66.592	45.239	
6 h		70.699	56.354	
9 h		76.319	17.192	
12 h		85.641	20.437	
24 h		83.777	12.967	
Untreated	S100A8	49.288	53.259	UBQC
3 h		60.613	81.107	
6 h		58.668	80.595	
9 h		68.549	79.379	
12 h		93.755	79.499	
24 h		104.646	74.031	
Untreated	MMP10	4.046	13.785	MMP2
3 h		7.276	13.155	
6 h		11.660	8.852	
9 h		31.218	25.606	
12 h		27.048	27.832	
24 h		27.002	47.613	

For densitometric analysis of PCR products IMAGE ANALYST software IMAGE J version 2.0 has been used.

have been previously described as NF-κB-responsive (16,36), and were found in our experiments to be maximally induced after 3 or 6 h of interleukin-1β treatment. This coincides with the time–course of the translocation of NF-κB into the nucleus (Fig. 1). Accordingly, promoters of most genes in clusters 1–4 (Fig. 2) contained at least one and up to six binding sites for NF-κB-related transcription factors (Table 1).

Genes modulated by interleukin-1β

To address the complex patterns of altered gene expression observed in our experiments, genes were classified into functional groups, which will be discussed in the following section in detail.

Cellular stress response

A number of heat-shock proteins were induced by interleukin-1β, including a 105-kDa heat-shock protein (HSPH1), several different isoforms of the 70-kDa heat-shock protein (HSPA1A, HSPA1L, HSPA2), a 90-kDa heat-shock protein (HSPCA), a 10-kDa heat-shock protein (HSPE1), and mitochondrial heat-shock protein 60 kDa. Most of these were placed in clusters I and III. Interestingly, the 60-kDa heat-shock protein is also expressed in epithelial cells from inflamed gingiva (37). Another interesting group of proteins involved in the cellular stress response are the metallothioneins. They protect cells from oxidative stress. We observed induction of metallothioneins -1E and -3 after 3–6 h of interleukin-1β treatment (cluster II). This finding corresponds with previous observations that increased levels of metallothioneins observed in smokers may reflect an attempt at defense against free radicals and inflammation in their gingiva. Inflammation is more extensive in the periodontal tissues of cigarette-smoking periodontitis patients than in non-smoking periodontitis patients (38).

DNA repair

Periodontal diseases are characterized in part by the generation of oxygen free radicals, which can cause breaks in cellular DNA strands. Therefore, the up-regulation of DNA repair enzymes, including topoisomerase II, is to be expected. However, no relevant observations have been published to date.

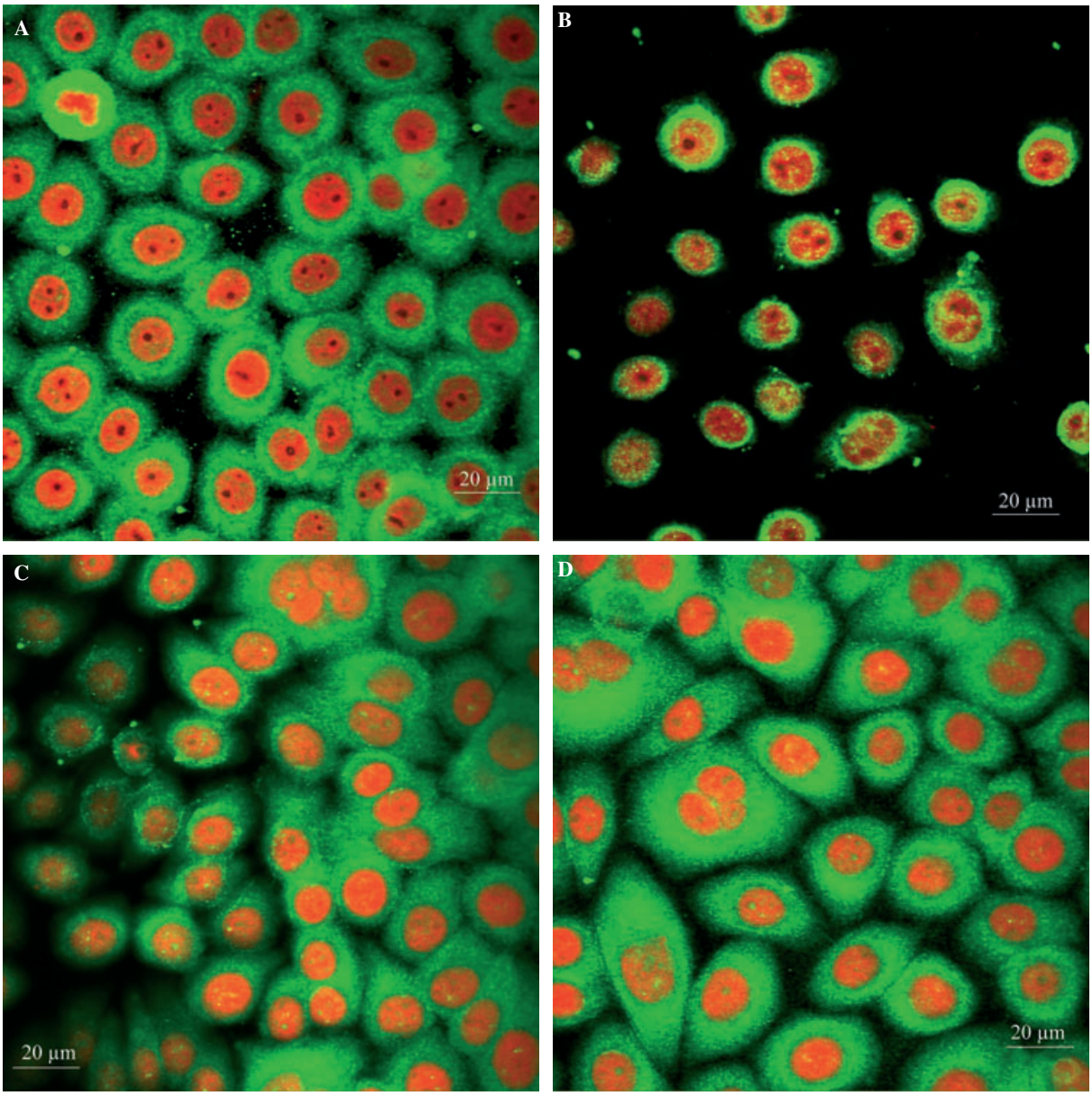

Fig. 1. Nuclear translocation of nuclear factor-κB (NF-κB) following treatment of IHGK with 200 U interleukin-1β. (A) In untreated cells NF-κB is mainly localized in the cytoplasm of the cells as indicated by the green fluorescence signal, while the red propidium iodide staining demarcates the cell nuclei. (B) After 6 h of treatment with interleukin-1β NF-κB shows a clear translocation to the nucleus visible in the mixed yellow fluorescence in the nuclear region and the cortical green fluorescence at the nucleus–cytoplasm interface. (C) 12 h after interleukin-1β treatment the green fluorescence signal showed a partial re-distribution in the cytoplasm. (D) After 24 h of interleukin-1β incubation an almost complete cytoplasmatic re-distribution of NF-κB was noted leading to an indirect immunofluorescence pattern similar to that in untreated cells. Bars represent 20 μm in A–D; all at same magnification.

Cell cycle and proliferation

Ornithine decarboxylase is a key enzyme of polyamine biosynthesis that is essential for growth-related cellular functions. Apart from its physiological role in cell proliferation, ornithine decarboxylase also contributes to the induction of apoptosis under certain conditions. Proliferating cell nuclear antigen, a valuable marker of cell proliferation, was induced by interleukin-1β after 3–6 h, which might indicate stimulation of cell proliferation. Simultaneously, we observed down-regulation of classic cell cycle-promoting genes, including cyclin B, cdc2, and centromer protein F. Therefore, more detailed analysis of the proliferative response of gingival keratinocytes to inflammatory processes is required.

Antipathogen response

We have identified a number of interleukin-1β responsive chemokines and

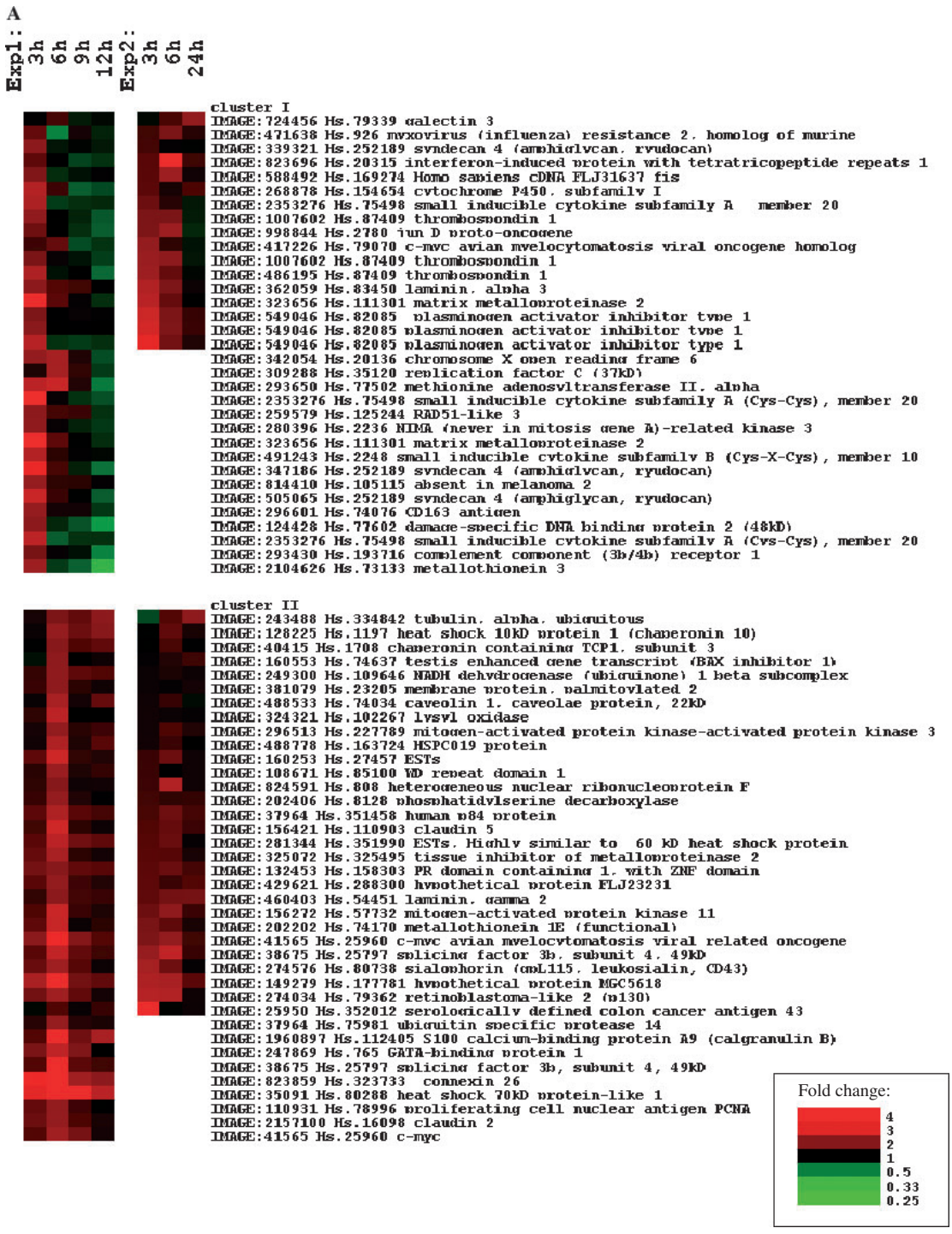

Fig. 2. Cluster analysis of mRNA gene transcription in IHGK following 200 U of interleukin-1β treatment. Data represent the median of four or six data-/gene points, obtained from two or three identical array hybridizations for each time-point, including duplicate spots, and from two completely independent sets of experiments. Data were filtered for genes that significantly change at any one given time-point of interleukin-1β treatment, logarithmically transformed (log base 2), and directly used for cluster analysis. Sorting of gene expression data was performed using the K-means algorithm, using seven preset clusters. The five time-points of the two microarray experiments of interleukin-1β stimulation are indicated at the top. Time-point one (both experiments) includes genes early modulated upon interleukin-1β incubation, i.e. 3 h. Time-points two, 6 h (both experiments), three 9 h (experiment 1), and four 12 h (experiment 1) describe an intermediate response. The fifth time-point, i.e. 24 h (experiment 2) denotes genes lately responding to interleukin-1β. Clusters of differentially expressed mRNAs obtained from experiments 1 and 2 (using a smaller microarray) are shown on the left, and IMAGE clones as well as IDs and gene names are given at the right. Color coding: green, down-regulation of gene expression; red, induction; black, no significant change.

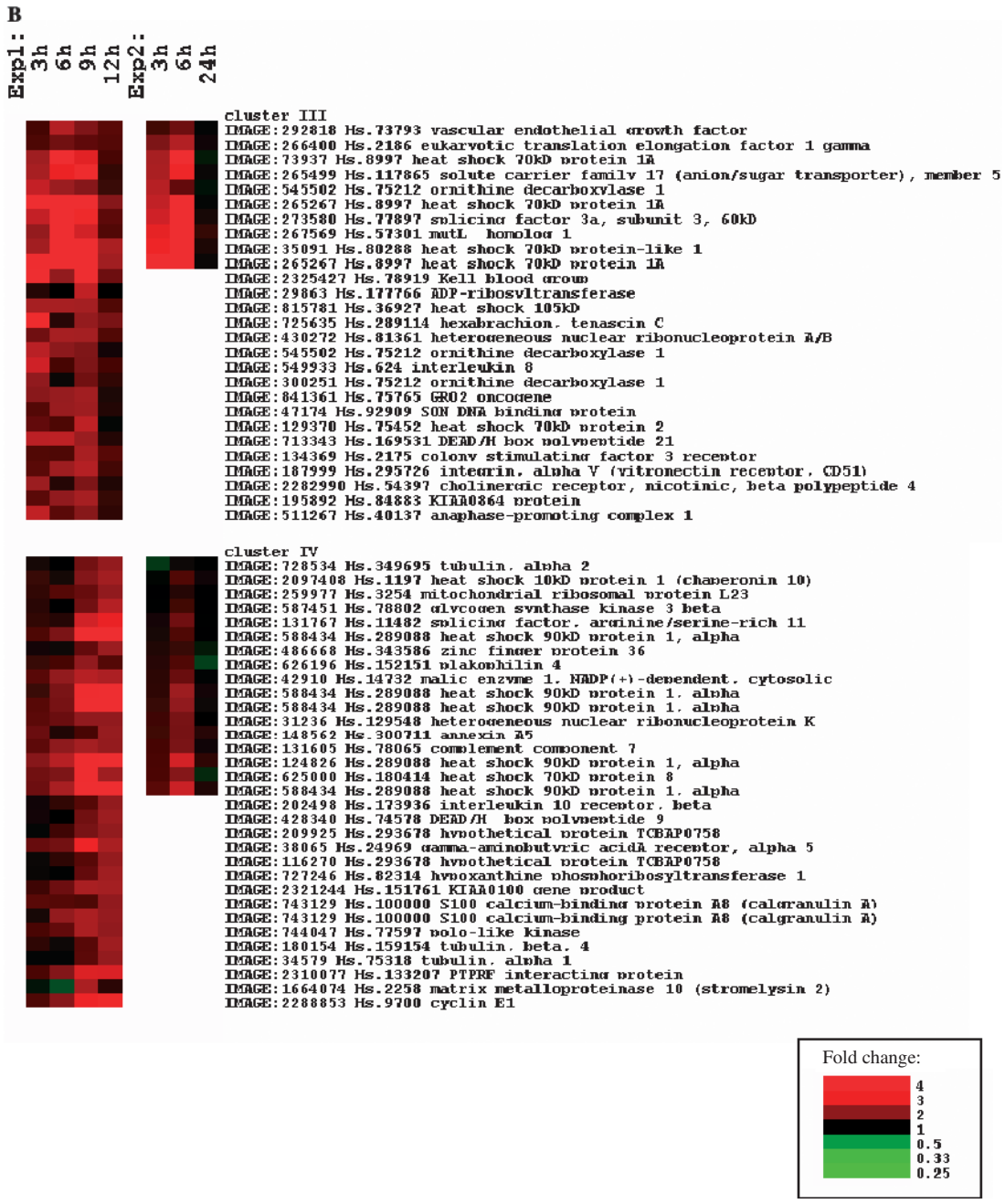

Fig. 2. (Continued)

cytokines, including interleukin-8. Both interleukin-6 and -8 are proinflammatory cytokines and are produced by keratinocytes. Previous studies have demonstrated the expression of interleukin-8 in periodontal tissues and keratinocytes *in vitro*. In addition, keratinocytes are a source of primary cytokines, including interleukin-1 and tumor necrosis factor-α, which show a strong synergistic effect on the production of interleukins -6 and -8 (39). Moreover, we have also identified the cytokines IP-10 (CXCL10, chemokine ligand 10) and MIP3a (CCL20, chemokine ligand 20) to be induced by interleukin-1β after 3–6 h. Similar findings, also including different cytokines, have been previously reported (40). MCP1 (CCL2, chemokine ligand 2), MIP1α (CCL3, chemokine ligand 3), MIP1β (CCL4, chemokine ligand 4), and IP-10 producing cells were found to be present in chronic inflammatory diseases including tooth granulomas. The chemokine ligands RANTES (CCL5, chemokine ligand 5), MIP1α and IP-10 were also reported to be elevated in inflamed periodontal tissues (41).

Extracellular matrix and matrix turnover of structural components

We observed pronounced alterations in genes involved in turnover of the

Fig. 2. (Continued)

extracellular matrix. For instance, fibronectin showed reduced expression levels upon interleukin-1β treatment. High concentrations of the cytokine interleukin-1β were shown to cause down-regulation of fibronectin transcripts in normal periodontal cells in tissue culture (42). In contrast, expression of tenascin C was induced by interleukin-1β. This glycoprotein plays an important role in the remodeling of the inflamed periodontal connective tissues and supports epithelial proliferation and migration. In our experiments, a number of different laminin isoforms was differentially expressed, suggesting profound rearrangements of the basal lamina. For instance, laminins α5 (*LAMA5*) and β1 (*LAMB1*) were down-regulated after 12 h, whereas laminins α3 (*LAMA3*) and γ2 (*LAMC2*) were induced rapidly after interleukin-1β stimulation. This finding confirms the observation that laminin 5 was poorly preserved in the basement membrane zone of inflamed gingival connective tissue (43). Similarly, perlecan (*HSPG2*) was down-regulated by IL-1β and showed reduced immunostaining in subepithelial and subendothelial basement membrane in periodontitis (43). Expression of syndecan 4 (*SDC4*) was induced after 3 h by IL-1β treatment, whereas expression of syndecan 3 (*SDC3*) was down-

Fig. 2. (Continued)

regulated after 12 h. These data suggest that modulation of syndecan expression contributes to cell migration in inflamed periodontium (44). Similar conclusions can be drawn from reduced expression of bullous pemphigoid antigen. In periodontitis, partial or complete absence of bullous pemphigoid antigen expression has been observed in the gingival basement membrane. As for changes in laminins and syndecan expression, loss of bullous pemphigoid antigen might contribute to enhanced motility and depth growth of junctional epithelial keratinocytes in inflamed tissues (45).

Matrix degradation

Alterated expression was found for a number of genes involved in matrix degradation. Plasmin activator inhibitor 1 (*SERPIN1*) was rapidly induced after interleukin-1β stimulation. Distribution of t-PA, u-PA, *SERPIN1* and

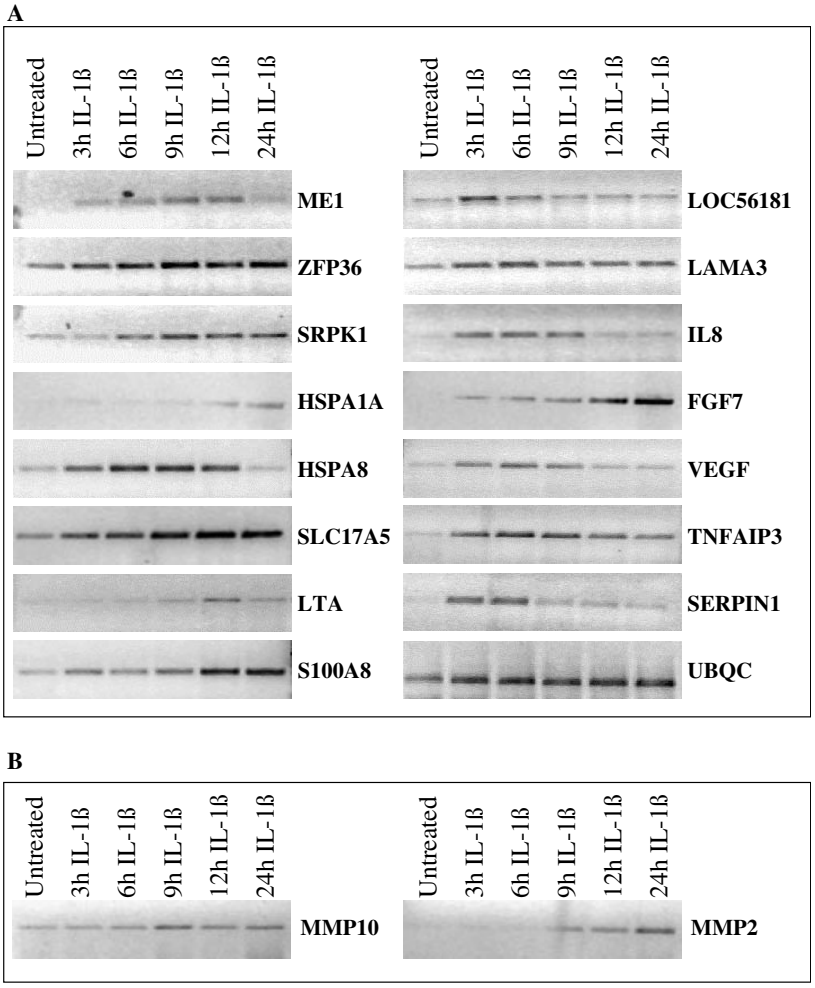

Fig. 3. (A) RT-PCR confirms modulation of transcription level of several interleukin-1β-responsive genes. IHGK were treated with 200 U of interleukin-1β for 3, 6, 12, and 24 h. Untreated cells served as controls. Abbreviations: ME malic enzyme; ZFP zinc finger protein 36; SRPK1 serine/arginine-rich protein specific kinase 1; HSPA1A heat-shock protein 70 kDa 1A; HSPA8 heat-shock protein 70 kDa 8; SLC17A5 solute carrier family 17, member 5; LTA lymphotoxin alpha; S100A8 calgranulin A; LOC56181 hypothetical protein RP1–317E23; LAMA3 kalinin; IL-8 interleukin 8; FGF7 keratinocyte growth factor; VEGF vascular endothelial growth factor; TNFAIP3 tumor necrosis factor-induced protein A20; SERPIN1 plasminogen activator inhibitor 1; UBQC ubiquitin C. (B) Modulation of matrix metalloproteinase (MMP) gene transcription, analyzed by RT-PCR. Gene transcription of MMP10 and -2 following 3, 6, 12, and 24 h of interleukin-1β stimulation (200 U). Untreated cells served as controls. Abbreviations: IL-1β interleukin-1β; MMP matrix metalloproteinase.

SERPIN2 have been observed around areas of inflammatory cell infiltration. Therefore, the plasminogen activator system may be influenced by the presence of proinflammatory interleukin-1β (46). Increased expression was also noted for matrix metalloproteinases, including MMP2 and MMP10 (Fig. 3B). Increased expression of MMP2, -7, -8, -13, and -14 was observed in gingival tissue specimens and gingival crevicular fluid from adult periodontitis patients and localized juvenile periodontitis patients when compared with healthy control tissue. In periodontal diseases several collagenolytic MMPs are over-expressed. This proteolytic cascade might be responsible for the tissue destruction characteristic of adult and juvenile periodontitis (47). As previously reported, inflammatory stages of periodontitis revealed up-regulation of α2, α3 and α6 integrins into the junctional and sulcular epithelial cells, which correlated with the stage of the periodontitis and the extent of the cellular infiltration (48). However, no induction of integrin αV (*ITGAV*) has been described so far.

Angiogenesis

Vascular endothelial growth factor (VEGF) and to a lesser extent the related VEGF-C, were induced by interleukin-1β, and are known to be involved in inflammation. VEGF was discussed as a potential factor in initiation and progression of gingivitis to periodontitis and could contribute to progression of the inflammation by promoting expansion of the vascular network (49).

In conclusion, our findings for the first time allow the characterization of a large number of genes that might be associated with oral inflammatory diseases, such as gingivitis and periodontitis. Among these, numerous genes previously described to be involved in these processes have been confirmed by our microarray experiments as well as novel genes have been identified. The genes described in this study might help to elucidate mechanisms underlying the onset, maintenance, and progression of periodontal diseases. Moreover, some of these genes, e.g. those genes associated with inflammation (*IL-8*), angiogenesis (*VEGF*), or turn-over of ECM (*SERPIN1*, *MMP2*, *MMP10*) may also represent potential candidate targets for future therapeutic intervention.

Acknowledgements

This work was supported by grants from the German Science Foundation (DFG to P.T., #198/1–1), which is part of the priority program #1086 'Genetic and molecular analysis of basement membranes and basement membrane anchorage', and the German Federal Ministry of Education and Research (BMBF) as part of the DHGP program.

References

1. O'Neill L. IL-1 versus TNF in arthritis? *Trends Immunol* 2001; **22:** 353–354.
2. Dinarello CA, Wolff SM. The role of interleukin-1 in disease. *N Engl J Med* 1993; **328:** 106–113.

3. Boch JA, Wara-aswapati N, Auron PE. Interleukin 1 signal transduction – current concepts and relevance to periodontitis. *J Dent Res* 2001; **80:** 400–407.
4. Alexander MB, Damoulis PD. The role of cytokines in the pathogenesis of periodontal disease. *Curr Opin Periodontol* 1994: 39–53.
5. Dinarello CA. Interleukin-1 beta, interleukin-18, and the interleukin-1 beta converting enzyme. *Ann N Y Acad Sci* 1998; **856:** 1–11.
6. Murphy JE, Robert C, Kupper TS. Interleukin-1 and cutaneous inflammation. a crucial link between innate and acquired immunity. *J Invest Dermatol* 2000; **114:** 602–608.
7. Ansel J, Perry P, Brown J, *et al.* Cytokine modulation of keratinocyte cytokines. *J Invest Dermatol* 1990; **94:** 101–107.
8. Dinarello CA. Biologic basis for interleukin-1 in disease. *Blood* 1996; **87:** 2095–2147.
9. Griswold DE, Connor JR, Dalton BJ *et al.* Activation of the IL-1 gene in UV-irradiated mouse skin: association with inflammatory sequelae and pharmacologic intervention. *J Invest Dermatol* 1991; **97:** 1019–1023.
10. Luger TA, Schwarz T. Evidence for an epidermal cytokine network. *J Invest Dermatol* 1990; **95:** 100–104.
11. Jefferies C, Bowie A, Brady G, Cooke EL, Li X, O'Neill LA. Transactivation by the p65 subunit of NF-kappaB in response to interleukin-1 (IL-1) involves MyD88, IL-1 receptor-associated kinase 1, TRAF-6, and Rac1. *Mol Cell Biol* 2001; **21:** 4544–4552.
12. Saklatvala J, Rawlinson LM, Marshall CJ, Kracht M. Interleukin 1 and tumour necrosis factor activate the mitogen-activated protein (MAP) kinase kinase in cultured cells. *FEBS Lett* 1993; **334:** 189–192.
13. Palsson EM, Popoff M, Thelestam M, O'Neill LA. Divergent roles for Ras and Rap in the activation of p38 mitogen-activated protein kinase by interleukin-1. *J Biol Chem* 2000; **275:** 7818–7825.
14. Ling L, Cao Z, Goeddel DV. NF-kappaB-inducing kinase activates IKK-alpha by phosphorylation of Ser- 176. *Proc Natl Acad Sci U S A* 1998; **95:** 3792–3797.
15. Foo SY, Nolan GP. NF-kappaB to the rescue: RELs, apoptosis and cellular transformation. *Trends Genet* 1999; **15:** 229–235.
16. Pahl HL. Activators and target genes of Rel/NF-kappaB transcription factors. *Oncogene* 1999; **18:** 6853–6866.
17. Parkos CA, Colgan SP, Diamond MS, *et al.* Expression and polarization of intercellular adhesion molecule-1 on human intestinal epithelia: consequences for CD11b/CD18–mediated interactions with neutrophils. *Mol Med* 1996; **2:** 489.
18. Kishimoto TK, Rothlein R. Extravasation. *Adv Pharmacol* 1994; **25:** 117–169.
19. Molinero LL, Fuertes MB, Girart MV, *et al.* NF-kappa B regulates expression of the MHC class I-related chain A gene in activated T lymphocytes. *J Immunol* 2004; **173:** 5583–5590.
20. Kojima H, Aizawa Y, Yanai Y, *et al.* An essential role for NF-kappa B in IL-18-induced IFN-gamma expression in KG-1 cells. *J Immunol* 1999; **162:** 5063–5069.
21. Seitz CS, Deng H, Hinata K, Lin Q, Khavari PA. Nuclear factor kappaB subunits induce epithelial cell growth arrest. *Cancer Res* 2000; **60:** 4085–4092.
22. Marionnet AV, Chardonnet Y, Viac J, Schmitt D. Differences in responses of interleukin-1 and tumor necrosis factor alpha production and secretion to cyclosporin-A and ultraviolet B-irradiation by normal and transformed keratinocyte cultures. *Exp Dermatol* 1997; **6:** 22–28.
23. Halbert CL, Demers GW, Galloway DA. The E7 gene of human papillomavirus type 16 is sufficient for immortalization of human epithelial cells. *J Virol*, 1991; **65:** 473–478.
24. Tomakidi P, Schuster G, Breitkreutz D, Kohl A, Ottl P, Komposch G. Organotypic cultures of gingival cells: an epithelial model to assess putative local effects of orthodontic plate and occlusal splint materials under more tissue-like conditions. *Biomaterials* 2000; **21:** 1549–1559.
25. Diehl F, Grahlmann S, Beier M, Hoheisel JD. Manufacturing DNA microarrays of high spot homogeneity and reduced background signal. *Nucleic Acids Res* 2001; **29:** E38.
26. Diehl F, Beckmann B, Kellner N, Hauser NC, Diehl S, Hoheisel JD. Manufacturing DNA microarrays from unpurified PCR products. *Nucleic Acids Res* 2002; **30:** e79.
27. Quandt K, Frech K, Karas H, Wingender E, Werner T. MatInd and MatInspector: new fast and versatile tools for detection of consensus matches in nucleotide sequence data. *Nucl Acids Res* 1995; **23:** 4878–4884.
28. Nees M, Geoghegan JM, Hyman T, Frank S, Miller L, Woodworth CD. Papillomavirus type 16 oncogenes downregulate expression of interferon-responsive genes and upregulate proliferation-associated and NF-kappaB-responsive genes in cervical keratinocytes. *J Virol* 2001; **75:** 4283–4296.
29. Eisen MB, Spellman PT, Brown PO, Botstein D. Cluster analysis and display of genome-wide expression patterns. *Proc Natl Acad Sci U S A* 1998; **95:** 14863–14868.
30. Nees M, Geoghegan JM, Munson P *et al.* Human papillomavirus type 16, E6 and E7 proteins inhibit differentiation–dependent expression of transforming growth factor–beta2 in cervical keratinocytes. *Cancer Res* 2000; **60:** 4289–4298.
31. Havard L, Rahmouni S, Boniver J, Delvenne P. High levels of p105 (NFKB1) and p100 (NFKB2) proteins in HPV16-transformed keratinocytes: role of E6 and E7 oncoproteins. *Virology* 2005; **331:** 357–366.
32. Ren Y, Savill J. Proinflammatory cytokines potentiate thrombospondin-mediated phagocytosis of neutrophils undergoing apoptosis. *J Immunol* 1995; **154:** 2366–2374.
33. Matsuzaki Y, Sugimoto H, Hamana K, Nagamine T, Matsuzaki S, Mori M. Effects of eicosanoids on lipopolysaccharide-induced ornithine decarboxylase activity and polyamine metabolism in the mouse liver. *J Hepatol* 1997; **27:** 193–200.
34. Kupper TS, Groves RW. The interleukin-1 axis and cutaneous inflammation. *J Invest Dermatol* 1995; **105:** 62–66.
35. Gemmell E, Seymour GJ. Cytokine profiles of cells extracted from humans with periodontal diseases. *J Dent Res* 1998; **77:** 16–26.
36. Karin M, Ben-Neriah Y. Phosphorylation meets ubiquitination. the control of NF-[kappa]B activity. *Annu Rev Immunol* 2000; **18:** 621–663.
37. Lundqvist C, Baranov V, Teglund S, Hammarstrom S, Hammarstrom ML. Cytokine profile and ultrastructure of intraepithelial gamma delta T cells in chronically inflamed human gingiva suggest a cytotoxic effector function. *J Immunol* 1994; **53:** 2302–2312.
38. Katsuragi H, Hasegawa A, Saito K. Distribution of metallothionein in cigarette smokers and non-smokers in advanced periodontitis patients. *J Periodontol* 1997; **68:** 1005–1009.
39. Fujisawa H, Wang B, Sauder DN, Kondo S. Effects of interferons on the production of interleukin-6 and interleukin-8 in human keratinocytes. *J Interferon Cytokine Res* 1997; **17:** 347–353.
40. Kabashima H, Yoneda M, Nagata K, Nonaka K, Hirofuji T, Maeda K. The presence of cytokine (IL-8, IL-1alpha, IL-1beta) -producing cells in inflamed gingival tissue from a patient manifesting Papillon–Lefèvre syndrome (PLS). *Cytokine* 2002; **18:** 121–126.
41. Gemmell E, Carter CL, Seymour GJ. Chemokines in human periodontal disease tissues. *Clin Exp Immunol* 2001; **125:** 134–141.
42. Parkar MH, Bakalios P, Newman HN, Olsen I. Expression and splicing of the fibronectin gene in healthy and diseased periodontal tissue. *Eur J Oral Sci* 1997; **105:** 264–270.
43. Haapasalmi K, Makela M, Oksala O *et al.* Expression of epithelial adhesion proteins and integrins in chronic inflammation. *Am J Pathol* 1995; **147:** 193–206.
44. Oksala O, Haapasalmi K, Hakkinen L, Uitto VJ, Larjava H. Expression of heparan sulphate and small dermatan/chondroitin sulphate proteoglycans in chronically inflamed human periodontium. *J Dent Res* 1997; **76:** 1250–1259.
45. Peng TK, Nisengard RJ, Levine MJ. The alteration in gingival basement membrane antigens in chronic periodontitis. *J Periodont* 1986; **57:** 20–24.
46. Xiao Y, Bunn CL, Bartold PM. Immunohistochemical demonstration of the plasminogen activator system in human gingival tissues and gingival fibroblasts. *J Periodontal Res* 1998; **33:** 17–26.
47. Tervahartiala T, Pirila E, Ceponis A *et al.* The in vivo expression of the collagenolytic matrix metalloproteinases (MMP-2, -8, -13, and -14) and matrilysin (MMP-7) in adult and localized juvenile periodontitis. *J Dent Res* 2000; **79:** 1969–1977.
48. Del Castillo LF, Schlegel Gomez R, Pelka M, Hornstein OP, Johannessen AC, von den Driesch P. Immunohistochemical localization of very late activation integrins in healthy and diseased human gingiva. *J Periodont Res* 1996; **31:** 36–42.
49. Johnson RB, Serio FG, Dai X. Vascular endothelial growth factors and progression of periodontal diseases. *J Periodontol* 1999; **70:** 848–852.